LINEAR FILTERING FOR NOISE REDUCTION AND INTERFERENCE REJECTION

Mehrez Souden, Jacob Benesty, and Sofiène Affes

INRS-ÉMT, 800, de la Gauchetière Ouest, Suite 6900, Montréal, H5A 1K6, QC, Canada.

{souden,benesty,affes}@emt.inrs.ca

ABSTRACT

We study the linearly constrained minimum variance (LCMV) and the minimum variance distortionless response (MVDR) filters when multiple interferers and unknown (ambient) noise coexist with a target speech signal. Precisely, the LCMV is designed to remove all the interference signals while preserving the desired speech and attempting to reduce the ambient noise components. The MVDR is simply formulated such that the overall ambient-noise-plus-interference are reduced while satisfying a distortionless constraint. We provide simplified expressions for both beamformers and show their relationship. Furthermore, we underline the limitations of the LCMV when the ambient noise is present. When the latter is absent, we also prove that the MVDR degenerates to the LCMV. Numerical examples are provided to support our study.

Index Terms— Noise reduction, interference rejection, microphone array, beamforming, linearly constrained minimum variance (LCMV), minimum variance distortionless response (MVDR).

1. INTRODUCTION

Microphone array signal processing has attracted a significant amount of research attention over the last few decades. Indeed, its inherent spatial aperture allows for additional key functions among which is the celebrated noise reduction with no speech distortion [1]–[10].

Earlier efforts devoted to gain insight into the functioning of multichannel noise reduction techniques include [11] where Bitzer et al. investigated the theoretical performance limits of the generalized sidelobe canceller (GSC) in the case of a spatially diffuse noise. In [12], Doclo and Moonen investigated the effect of gain and phase errors in microphone arrays on broadband beamforming and proposed robust design procedures of beamformers. In [13], the theoretical equivalence between the LCMV and its GSC counterpart was demonstrated. In [8], Habets et al. studied the effectiveness of the MVDR when designed to remove both additive noise and reverberation. It was found that a tradeoff between noise reduction and dereverberation has to be made. However, dereverberation still remains an open field for future research and we would rather focus on noise reduction here. Another notable effort to understand the functioning of the multichannel linear processing for noise reduction was published in [10]. Therein, Gannot and Cohen studied the noise reduction ability of the channel transfer function (TF) ratios-based GSC beamformer in [10]. They found that it is theoretically possible to achieve infinite noise reduction when only one spatially coherent noise overlaps with the desired speech. In [5, 6], analytical results showing the tradeoff between noise reduction and speech distortion in the parameterized multichannel Wiener filtering were established.

In this paper, we are interested in the analysis of the potential of microphone arrays to reduce the ambient noise and reject multiple interferers when both types of signals overlap with a target speech. A widely known example consists in teleconferencing environments where hands-free full-duplex communication devices are deployed for speech acquisition. In this situation, the target signal is generated by one speaker while the interference is more likely to be generated by other participants or devices located within the same enclosure. In addition, ambient noise is ubiquitous in these environments and it has to be considered. The proposed study is motivated by the need to understand the pros and cons of two main beamformers that are commonly utilized in this scenario: the MVDR that simultaneously reduces overall interference-plus-ambient-noise energy and the LCMV that totally rejects all the interferers while attempting to reduce the ambient noise. Both filters preserve the target speech signal as well.

2. DATA MODEL AND ASSUMPTIONS

We consider the following frequency domain representation of the investigated data model [9]

$$Y_n(j\omega) = G_n(j\omega)S(j\omega) + \sum_{l=1}^{L} D_{n,l}(j\omega)\Psi_l(j\omega) + V_n(j\omega), \quad (1)$$

where $Y_n(j\omega)$, $G_n(j\omega)$, $S(j\omega)$, $D_{n,l}(j\omega)$, $\Psi_l(j\omega)$, and $V_n(j\omega)$ are discrete-time Fourier transforms of the output of microphone n ($n = 1, ..., N$), the channel TF between the target source and microphone n, the channel TF between the lth interfering source and microphone n, the target speech signal, the original lth interference signal, and the ambient noise component seen by microphone n, respectively. Also, we define $X_n(j\omega) = G_n(j\omega)S(j\omega)$, $I_{n,l}(j\omega) = D_{n,l}(j\omega)\Psi_l(j\omega)$ for $l = 1, ..., L$, and $I_n(j\omega) = \sum_{l=1}^{L} I_{n,l}(j\omega)$. From now on, the frequency dependence will be removed for the sake of clarity.

Our aim is to recover one of the noise-free speech components, say X_1, the best way we can (along some criteria to be defined later) by applying a linear filter $\mathbf{h}$ to the overall observation vector $\mathbf{y} = [Y_1\ Y_2\ \cdots\ Y_N]^T$. $(\cdot)^T$ denotes the transpose operator. For notational convenience, we also define $\mathbf{x}$, $\mathbf{i}$, and $\mathbf{v}$ as $\mathbf{y}$ and $\mathbf{w} = \mathbf{v} + \mathbf{i}$. The output of $\mathbf{h}$ is

$$\begin{aligned} Z &= \mathbf{h}^H\mathbf{y} \\ &= \mathbf{h}^H\mathbf{x} + \mathbf{h}^H\mathbf{i} + \mathbf{h}^H\mathbf{v}, \end{aligned} \quad (2)$$

where $\mathbf{h}^H\mathbf{x}$ is the filtered speech component, $\mathbf{h}^H\mathbf{i}$ is the residual interference part, $\mathbf{h}^H\mathbf{v}$ is the residual noise, and $(\cdot)^H$ is the transpose-conjugate operator. The vector containing all the channel TFs between the desired source and microphones' locations is defined as $\mathbf{g} = [G_1\ G_2\ ...\ G_N]^T$, while $\mathbf{D} = [\mathbf{d}_1\ \mathbf{d}_2\ ...\ \mathbf{d}_L]$ is the $N \times L$ matrix where $\mathbf{d}_l = [D_{1,l}\ D_{2,l}\ ...\ D_{N,l}]^T$ is the vector containing all the channel TFs associated with the lth interferer. Also, we define $\phi_{aa} = E\{AA^*\}$ and $\mathbf{\Phi}_{aa} = E\{\mathbf{a}\mathbf{a}^H\}$, respectively, as the PSD and PSD matrix of a given random process A and a vector of random processes $\mathbf{a}$. We assume that all the interferers are uncorrelated which means that $\mathbf{\Phi}_{\psi\psi} = \mathrm{diag}[\phi_{\psi_1\psi_1}\ \phi_{\psi_2\psi_2}\ ...\ \phi_{\psi_L\psi_L}]$.

978-1-4244-4296-6/10/$25.00 ©2010 IEEE

As performance measures, we use the SNR and SIR at the output of a given filter $\mathbf{h}$ which are defined as $\mathrm{SNR_o}(\mathbf{h}) = \frac{\mathbf{h}^H \mathbf{\Phi}_{xx}\mathbf{h}}{\mathbf{h}^H \mathbf{\Phi}_{vv}\mathbf{h}}$ and $\mathrm{SIR_o}(\mathbf{h}) = \frac{\mathbf{h}^H \mathbf{\Phi}_{xx}\mathbf{h}}{\mathbf{h}^H \mathbf{\Phi}_{ii}\mathbf{h}}$. In our processing, we are only interested in reducing the additive noise $\mathbf{w}$ as in [4, 5, 6, 7, 9, 10] in contrast to [3, 8]. Thus, we take the first microphone as a reference and accordingly define the input $\mathrm{SNR} = \frac{\phi_{x_1x_1}}{\phi_{v_1v_1}}$ and input $\mathrm{SIR} = \frac{\phi_{x_1x_1}}{\phi_{i_1i_1}}$.

3. MINIMUM VARIANCE DISTORTIONLESS RESPONSE

The optimization problem leading to the MVDR noise reduction filter is known as [1, 4, 5, 6, 7, 10]

$$\mathbf{h}_{\mathrm{MVDR}} = \arg\min_{\mathbf{h}} \mathbf{h}^H \mathbf{\Phi}_{ww}\mathbf{h} \quad \text{subject to} \quad \mathbf{g}^H\mathbf{h} = G_1^*. \tag{3}$$

The MVDR solution is then written as

$$\mathbf{h}_{\mathrm{MVDR}} = G_1^* \frac{\mathbf{\Phi}_{ww}^{-1}\mathbf{g}}{\mathbf{g}^H \mathbf{\Phi}_{ww}^{-1}\mathbf{g}}. \tag{4}$$

We use the following matrix inversion lemma

$$\mathbf{\Phi}_{ww}^{-1} = \mathbf{\Phi}_{vv}^{-1} - \mathbf{\Phi}_{vv}^{-1}\mathbf{D}\left(\mathbf{\Phi}_{\psi\psi}^{-1} + \mathbf{D}^H\mathbf{\Phi}_{vv}^{-1}\mathbf{D}\right)^{-1}\mathbf{D}^H\mathbf{\Phi}_{vv}^{-1}$$

to obtain

$$\mathbf{h}_{\mathrm{MVDR}} = G_1^* \frac{\mathbf{P}\mathbf{g}}{\mathbf{g}^H\mathbf{P}\mathbf{g}}, \tag{5}$$

where $\mathbf{P} = \mathbf{\Phi}_{ww}^{-1}$. Since we are only interested in noise reduction, it is possible to directly use the noise and noisy data statistics to implement the above expression as [1, 5, 6]

$$\mathbf{h}_{\mathrm{MVDR}} = \frac{\left[\mathbf{\Phi}_{ww}^{-1}\mathbf{\Phi}_{yy} - \mathbf{I}\right]\mathbf{u}_1}{\mathrm{tr}\left[\mathbf{\Phi}_{ww}^{-1}\mathbf{\Phi}_{yy}\right] - N}, \tag{6}$$

where $\mathbf{u}_1 = [1\ 0\ ...\ 0]^T$ is an N-dimensional vector. In the sequel, we will be interested in the analysis of the MVDR's behavior with respect to both interference and ambient noise components that can be better seen using (5).

4. LINEARLY CONSTRAINED MINIMUM VARIANCE

Here, the LCMV beamformer that we are interested in aims at rejecting all the interferers while preserving the target signal and attempting to reduce the ambient noise. Mathematically, we have the following optimization problem [2, 9]

$$\mathbf{h}_{\mathrm{LCMV}} = \arg\min_{\mathbf{h}} \mathbf{h}^H \mathbf{\Phi}_{vv}\mathbf{h} \quad \text{subject to} \quad \mathbf{C}^H\mathbf{h} = G_1^*\tilde{\mathbf{u}}_1, \tag{7}$$

where $\tilde{\mathbf{u}}_1 = [1\ 0\ ...\ 0]^T$ is an $(L+1)$–dimensional vector, and $\mathbf{C} = [\mathbf{g}\ \mathbf{D}]$. The solution to this optimization problem is known as [9, 13]

$$\mathbf{h}_{\mathrm{LCMV}} = G_1^*\mathbf{\Phi}_{vv}^{-1}\mathbf{C}\left[\mathbf{C}^H\mathbf{\Phi}_{vv}^{-1}\mathbf{C}\right]^{-1}\mathbf{u}_1. \tag{8}$$

This form is not easy to interpret. Nevertheless, we can prove that (8) can be written as (see Appendix)

$$\mathbf{h}_{\mathrm{LCMV}} = G_1^* \frac{\mathbf{Q}\mathbf{g}}{\mathbf{g}^H\mathbf{Q}\mathbf{g}}, \tag{9}$$

where

$$\mathbf{Q} = \mathbf{\Phi}_{vv}^{-1} - \mathbf{\Phi}_{vv}^{-1}\mathbf{D}\left(\mathbf{D}^H\mathbf{\Phi}_{vv}^{-1}\mathbf{D}\right)^{-1}\mathbf{D}^H\mathbf{\Phi}_{vv}^{-1}. \tag{10}$$

It is interesting to see how similar both expressions (5) and (9) are. Indeed, they only differ by the choice of the projection-like matrix $\mathbf{P}$ or $\mathbf{Q}$. Further interpretations are given below.

5. PERFORMANCE ANALYSIS

In order to understand the behaviors of both filters and outline their relationship, we consider the cases of spatially white ambient noise and single interferer ($L = 1$).

Spatially White Ambient Noise: In this scenario, the PSD matrix of the ambient noise is given by $\mathbf{\Phi}_{vv} = \sigma^2\mathbf{I}$ where σ^2 is the noise power. Consequently, the MVDR is expressed as

$$\mathbf{h}_{\mathrm{MVDR}} = G_1^* \frac{\mathbf{I} - \mathbf{D}\left(\sigma^2\mathbf{\Phi}_{\psi\psi}^{-1} + \mathbf{D}^H\mathbf{D}\right)^{-1}\mathbf{D}^H}{\mathbf{g}^H\left[\mathbf{I} - \mathbf{D}\left(\sigma^2\mathbf{\Phi}_{\psi\psi}^{-1} + \mathbf{D}^H\mathbf{D}\right)^{-1}\mathbf{D}^H\right]\mathbf{g}}\mathbf{g}, \tag{11}$$

while the LCMV's expression becomes

$$\mathbf{h}_{\mathrm{LCMV}} = G_1^* \frac{\mathbf{I} - \mathbf{D}\left(\mathbf{D}^H\mathbf{D}\right)^{-1}\mathbf{D}^H}{\mathbf{g}\left[\mathbf{I} - \mathbf{D}\left(\mathbf{D}^H\mathbf{D}\right)^{-1}\mathbf{D}^H\right]\mathbf{g}}\mathbf{g}. \tag{12}$$

We see from (11) and (12) that the LCMV performs a projection[1] onto the subspace orthogonal to the L-dimensional one spanned by the columns of $\mathbf{D}$ regardless of the level of the ambient noise, i.e., σ^2, and interferers, i.e., $\mathbf{\Phi}_{\psi\psi}$. Conversely, the MVDR takes into account the energy terms by modifying the projection matrix by a term $\sigma^2\mathbf{\Phi}_{\psi\psi}^{-1} = \mathrm{diag}\left[\frac{1}{\mathrm{INR}_1}\ ...\ \frac{1}{\mathrm{INR}_L}\right]$, where we define $\mathrm{INR}_l = \frac{\phi_{\psi_l\psi_l}}{\sigma^2}$ as the lth interference-to-ambient-noise ratio. If we further assume that the interferers have equal energies, i.e., $\mathrm{INR}_1 = \mathrm{INR}_2 = \cdots \mathrm{INR}_L = \mathrm{INR}$, and suppose that $\mathrm{INR} \to \infty$ (equivalently supposing that $\sigma^2 \to 0$ for given levels of interference)

$$\lim_{\mathrm{INR}\to\infty} \mathbf{h}_{\mathrm{MVDR}} = \mathbf{h}_{\mathrm{LCMV}}. \tag{13}$$

This result means that the MVDR (with its simple and efficient formulation) is able to perform perfect source extraction from a mixture of multiple competing speakers. Resorting to the LCMV may not be justified if we consider the required knowledge of the all propagation paths of the interferers and potential amplification of ambient noise that will be shown below. When the energy of the interferers is too low as compared to the ambient noise, we have

$$\lim_{\mathrm{INR}\to 0} \mathbf{h}_{\mathrm{MVDR}} = G_1^* \frac{\mathbf{g}}{\|\mathbf{g}\|^2}, \tag{14}$$

which is the matched beamformer that coherently adds up the signal components to enhance the desired signal and attenuate the ambient noise.

Single Interferer: In this scenario, we have shown in [7] that the MVDR can be written as a linear combination of the LCMV (totally focussed on interference removal) and a matched filter (totally focussed on ambient noise removal) and allows for a certain tradeoff between both functions by properly weighting both components depending on the INR. The decomposition in [7] is a particular case of (5) even though no simplified decomposition is available when multiple interferers are present. However, one can expect a similar behavior where all the interferers locations and energies are taken into account by the MVDR. The analysis of the single interferer scenario seems to be sufficient and very insightful. For the sake of simplicity here, we further assume that the ambient noise is white and that the environment is anechoic. Consequently, the SIR and SNR at the output of the LCMV and MVDR filters are given by [7]

$$\mathrm{SNR_o}(\mathbf{h}_{\mathrm{MVDR}}) = \frac{N}{1 + \frac{N^2\ \mathrm{INR}^2\kappa(1-\kappa)}{[1+N\ \mathrm{INR}(1-\kappa)]^2}}\mathrm{SNR}, \tag{15}$$

[1] At the same time, no distortion is introduced to the desired signal.

$$\mathrm{SIR_o}\left(\mathbf{h}_{\mathrm{MVDR}}\right) = \frac{\left[1 + N\,\mathrm{INR}\left(1-\kappa\right)\right]^2}{\kappa}\mathrm{SIR}, \quad (16)$$

$$\mathrm{SNR_o}\left(\mathbf{h}_{\mathrm{LCMV}}\right) = N\left(1-\kappa\right)\mathrm{SNR}, \quad (17)$$

$$\mathrm{SIR_o}\left(\mathbf{h}_{\mathrm{LCMV}}\right) = +\infty, \quad (18)$$

where $\kappa = \frac{|\mathbf{g}^H\mathbf{d}|^2}{\|\mathbf{g}\|^2\|\mathbf{d}\|^2}$ is the collinearity factor that has a critical effect on the performance of both beamformers. Essentially, when this factor is increased toward 1, an amplified ambient noise can be obtained at the output of the LCMV (i.e., $\frac{\mathrm{SNR_o}(\mathbf{h}_{\mathrm{LCMV}})}{\mathrm{SNR}} = N\left(1-\kappa\right) < 1$). The MVDR can also amplify the ambient noise if the input INR and collinearity factor are sufficiently high (in this case, the ambient noise level takes very small value and its amplification is not disastrous as it may be the case for the LCMV that may dramatically amplify it regardless of its energy).

When multiple interferers are present, the likelihood of having one of them in the vicinity of the target source signal becomes higher. Consequently, it is more likely that the ambient noise becomes amplified, especially by the LCMV. In addition, the estimation of the channel TFs associated with the interferences becomes more and more complicated. Conversely, the MVDR allows for blind interference and ambient noise removal since the knowledge of the channel TFs of the interferers is not required as shown in (6) where only the PSD matrices of the interference-plus-ambiant-noise and noisy data are used.

6. NUMERICAL EXAMPLE

For illustration purposes, we consider a uniform linear array (ULA) of 4 microphones with δ being the inter-microphone spacing, located in a reverberant enclosure. The microphone elements are placed on the axis ($y_0 = 1.016, z_0 = 1.016$) m with the center of the array being at ($x_0 = 1.524$ m$, y_0, z_0$) and the nth microphone at $(x_0 - \frac{N-2n+1}{2}\delta, y_0, z_0)$ with $n = 1, ..., N$. In the first example, we consider the case of an anechoic room ($T_{60} = 0$ ms) where the channel transfer functions are pure delay-based. In the second scenario, we consider a reverberant enclosure simulated using the image method [14] with a reverberation time $T_{60} = 300$ ms. The source and the two interferers are located in the same enclosure at a distance 2.5 m away from the array center and at the azimuthal angles $\theta_s = 90^\circ$, $\theta_{i_1} = \theta_s - \Delta\theta$ and $\theta_{i_2} = \theta_s + \Delta\theta$ which are measured counter-clockwise from the array axis. $\Delta\theta$ will be chosen depending on the examples investigated below. An additive spatially white noise was added to model the ambient noise. We choose the input SIR and SNR to be equal to -3 dB and 0 dB, respectively.

In the first setup, we investigate the effect of the angular separation $\Delta\theta$ on the performance of the MVDR and LCMV beamformers at a frequency $f = 1$ kHz. The inter-microphones spacing is set such that $\delta = \frac{c}{2f}$ ($c = 343$ ms^{-1} is the speed of sound). Figs. 1 (a) and (b) show the effect of $\Delta\theta$ on the SIR and SNR at the output of both beamformers. When $\Delta\theta$ decreases, the output SNR of the LCMV is decreased. It is even much lower than the input SNR for $\Delta\theta < 15^\circ$. In contrast, the output SNR of the MVDR is almost unaffected while very low output SIR values are obtained for small $\Delta\theta$. To gain a better understanding of these results, we provide the normalized beampatterns of both beamformers in Fig. 2 for $\Delta\theta = 30^\circ$ and 10°. We see that when $\Delta\theta$ is small, two major behaviors of the LCMV emerge: displacement of the main beam away from the source location and appearance of sidelobes. The MVDR's beampattern also exhibits larger sidelobes when $\Delta\theta$ is decreased. To explain these behaviors, recall that in the formulation of the optimization problems leading to the LCMV and MVDR, the array response towards the source direction is forced to the unity gain. This constraint is always satisfied (the maxima of the LCMV beampattern correspond to values larger than one and the results presented in Fig. 2 are normalized with respect to the largest value). When the interferers move towards the target source, it becomes harder for the LCMV to satisfy two contradictory constraints: switching the array gain from zero to one. This fact causes some instabilities that translate into the appearance of sidelobes and displacement of the maximum far from the interference, thereby leading the array to capture the ambient noise which spans the whole space. Finally, it is obvious that when $\Delta\theta$ increases, the two filters perform relatively well in terms of noise (for the LCMV) and interference (for the MVDR) removal. In the second setup, we consider a reverberant enclosure and show the resulting output SNR and SIR for $\Delta\theta = 30^\circ$ and 10° for the frequency span 0 to 4 kHz in Fig. 3. We notice that the infinite SIR gain achieved by the LCMV may come at the price of very low output SNR as compared to the MVDR, especially for the low frequency range (lower than 1000 Hz). When we compare Figs. 3 (a) and (c) to Figs. 3 (b) and (d), respectively, we notice that when the interference is placed near the target source, a remarkable performance degradation is observed in terms of output SNR, especially for the LCMV filter, and in terms of output SIR for the MVDR.

7. CONCLUSIONS

In this paper, we studied the ability of the MVDR and LCMV beamformers to simultaneously reduce the ambiant noise and reject the multiple interferers when both types of signals overlap to the target speech signal. We elaborated simplified expressions for both beamformers to illustrate the tradeoff of noise reduction and interference rejection. Specifically, while the LCMV totally focusses on interference rejection and may dramatically increase the ambiant noise, the MVDR seems to be more promising since it tradeoffs both functions by taking into account the energies of both types of signals. In the particular case where the ambient noise is weak (as compared to the level of the interferers), the MVDR is more focussed on interference rejection and degenerates to the LCMV without requiring the knowledge of the channel TFs associated to the interferers. Conversely, when the interferers are weak (as compared to the ambient noise), the MVDR allows for better ambient noise reduction in contrast to the LCMV.

APPENDIX: PROOF OF THE NEW LCMV EXPRESSION

In order to prove (9)–(10), we first see that

$$\mathbf{C}^H\boldsymbol{\Phi}_{vv}^{-1}\mathbf{C} = \begin{bmatrix} \mathbf{g}^H\boldsymbol{\Phi}_{vv}^{-1}\mathbf{g} & \mathbf{g}^H\boldsymbol{\Phi}_{vv}^{-1}\mathbf{D} \\ \mathbf{D}^H\boldsymbol{\Phi}_{vv}^{-1}\mathbf{g} & \mathbf{D}^H\boldsymbol{\Phi}_{vv}^{-1}\mathbf{D} \end{bmatrix}. \quad (19)$$

By using (19), we can compute (20) that we plug into (8) to obtain (21). Finally, we use the matrix inversion lemma to expand $\left(\mathbf{g}^H\boldsymbol{\Phi}_{vv}^{-1}\mathbf{g}\mathbf{D}^H\boldsymbol{\Phi}_{vv}^{-1}\mathbf{D} - \mathbf{D}^H\boldsymbol{\Phi}_{vv}^{-1}\mathbf{g}\mathbf{g}^H\boldsymbol{\Phi}_{vv}^{-1}\mathbf{D}\right)^{-1}$ and use it in (21) to obtain the LCMV expression in (9)–(10).

$$\left(\mathbf{C}^H\boldsymbol{\Phi}_{vv}^{-1}\mathbf{C}\right)^{-1}\mathbf{u}_1 = \quad (20)$$
$$\begin{bmatrix} \left\{\mathbf{g}^H\boldsymbol{\Phi}_{vv}^{-1}\mathbf{g} - \mathbf{g}^H\boldsymbol{\Phi}_{vv}^{-1}\mathbf{D}\left(\mathbf{D}^H\boldsymbol{\Phi}_{vv}^{-1}\mathbf{D}\right)^{-1}\mathbf{D}^H\boldsymbol{\Phi}_{vv}^{-1}\mathbf{g}\right\}^{-1} \\ -\left\{\mathbf{g}^H\boldsymbol{\Phi}_{vv}^{-1}\mathbf{g}\mathbf{D}^H\boldsymbol{\Phi}_{vv}^{-1}\mathbf{D} - \mathbf{D}^H\boldsymbol{\Phi}_{vv}^{-1}\mathbf{g}\mathbf{g}^H\boldsymbol{\Phi}_{vv}^{-1}\mathbf{D}\right\}^{-1}\mathbf{D}^H\boldsymbol{\Phi}_{vv}^{-1}\mathbf{g} \end{bmatrix},$$

$$\frac{\mathbf{h}_{\text{LCMV}}}{G_1^*} = \frac{\mathbf{\Phi}_{vv}^{-1}\mathbf{g}}{\mathbf{g}^H\mathbf{\Phi}_{vv}^{-1}\mathbf{g} - \mathbf{g}^H\mathbf{\Phi}_{vv}^{-1}\mathbf{D}\left(\mathbf{D}^H\mathbf{\Phi}_{vv}^{-1}\mathbf{D}\right)^{-1}\mathbf{D}^H\mathbf{\Phi}_{vv}^{-1}\mathbf{g}} \quad (21)$$

$$-\mathbf{\Phi}_{vv}^{-1}\mathbf{D}\left(\mathbf{g}^H\mathbf{\Phi}_{vv}^{-1}\mathbf{g}\mathbf{D}^H\mathbf{\Phi}_{vv}^{-1}\mathbf{D} - \mathbf{D}^H\mathbf{\Phi}_{vv}^{-1}\mathbf{g}\mathbf{g}^H\mathbf{\Phi}_{vv}^{-1}\mathbf{D}\right)^{-1}\mathbf{D}^H\mathbf{\Phi}_{vv}^{-1}\mathbf{g}.$$

8. REFERENCES

[1] J. Benesty, J. Chen, and Y. Huang, *Microphone Array Signal Processing*. Springer-Verlag, Berlin, Germany, 2008.

[2] J. Benesty, J. Chen, Y. Huang, and J. Dmochowski, "On microphone-array beamforming from a MIMO acoustic signal processing perspective," *IEEE Trans. Audio, Speech, Language Process.,* vol. 15, pp. 1053–1065, Mar. 2007.

[3] S. Affes and Y. Grenier, "A signal subspace tracking algorithm for microphone array processing of speech," *IEEE Trans. Speech, Audio Process.*, vol. 5, pp. 425–437, Sept. 1997.

[4] S. Gannot, D. Burshtein, and E. Weinstein, "Signal enhancement using beamforming and nonstationarity with applications to speech," *IEEE Trans. Signal Process.*, vol. 49, pp. 1614–1626, Aug. 2001.

[5] M. Souden, J. Benesty, and S. Affes, "New insights into non-causal multichannel linear filtering for noise reduction," in *Proc. IEEE ICASSP*, 2009, pp. 141–144.

[6] M. Souden, J. Benesty, and S. Affes, "On optimal frequency-domain multichannel linear filtering for noise reduction," *IEEE Trans. Audio, Speech, Language Process.,* vol. 18, pp. 260–276, Feb. 2010.

[7] M. Souden, J. Benesty, and S. Affes, "On optimal beamforming for noise reduction and interference rejection," in *Proc. IEEE WASPAA*, 2009, pp. 109–112.

[8] E. Habets, J. Benesty, I. Cohen, and S. Gannot, "New insights into the MVDR beamformer in room acoustics," *IEEE Trans. Audio, Speech, Language Process.,* vol. 18, pp. 158–170, Jan. 2010.

[9] S. Markovich, S. Gannot, and I. Cohen, "Multichannel eigenspace beamforming in a reverberant noisy environment with multiple interfering speech signals," *IEEE Trans. Audio, Speech, Language Process.* vol. 17, no. 6, pp. 1071–1086,Aug. 2009.

[10] S. Gannot and I. Cohen, "Adaptive beamforming and postfiltering," in *Springer Handbook of Speech Processing*, J. Benesty, M.M. Sondhi, and Y. Huang, editors, Springer-Verlag, 2007, Chapter 47, pp. 945–978.

[11] J. Bitzer, K.U. Simmer, and K.-D. Kammeyer, "Theoretical noise reduction limits of the generalized sidelobecanceller (GSC) for speech enhancement," in *Proc. IEEE ICASSP*, 1999, vol. 5, pp. 2965–2968.

[12] S. Doclo and M. Moonen, "Design of broadband beamformers robust against gain and phase errors in the microphone array characteristics," *IEEE Trans. Signal Process.,* vol. 51, pp. 2511–2526, Oct. 2003.

[13] B. R. Breed and J. Strauss, "A short proof of the equivalence of LCMV and GSC beamforming," *IEEE Signal Process. Lett.*, vol. 9, pp. 168–169, Jun. 2002.

[14] J.B. Allen and D.A. Berkley, "Image method for efficiently simulating small-room acoustics," *J. Acoust. Soc. Amer.*, vol. 65, pp. 943–950, Apr. 1979.

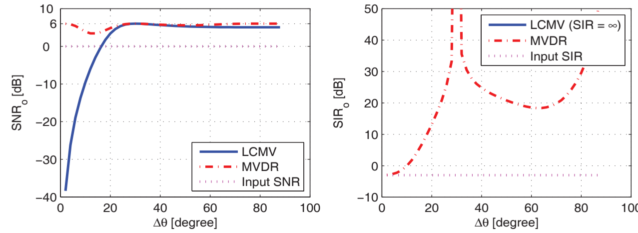

(a) Output SNR (b) Output SIR

Fig. 1. Performance of the MVDR and LCMV vs. $\Delta\theta$: anechoic room.

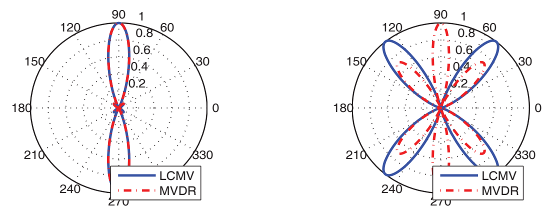

(a) $\Delta\theta = 30^\circ$ (b) $\Delta\theta = 10^\circ$

Fig. 2. Beampatterns of the MVDR and LCMV filters; the source is at 90° and two interferences at $90^\circ \pm \Delta\theta$: anechoic room.

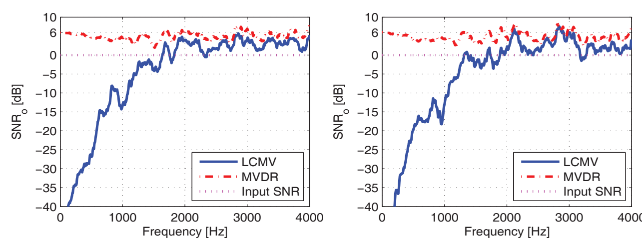

(a) $\Delta\theta = 30^\circ$ (b) $\Delta\theta = 10^\circ$

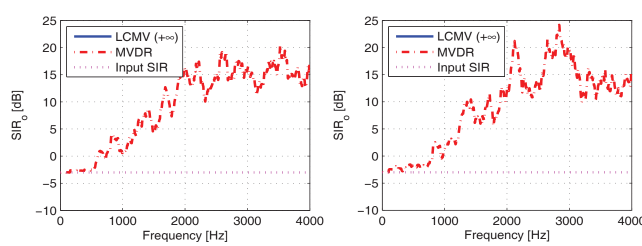

(c) $\Delta\theta = 30^\circ$ (d)$\Delta\theta = 10^\circ$

Fig. 3. SNR and SIR at the output of the LCMV and MVDR filters: reverberant room.